Physics Letters B 784 (2018) 277–283

Contents lists available at ScienceDirect

Physics Letters B

www.elsevier.com/locate/physletb

Experimental and theoretical study of deuteron–proton elastic scattering for proton kinetic energies between $T_p = 882.2$ MeV and $T_p = 918.3$ MeV

C. Fritzsch [a,*], S. Barsov [b], I. Burmeister [a], S. Dymov [c,d], R. Gebel [c], M. Hartmann [c], A. Kacharava [c], A. Khoukaz [a], V. Komarov [d], V.I. Kukulin [e], P. Kulessa [f], A. Kulikov [d], A. Lehrach [c], B. Lorentz [c], D. Mchedlishvili [c,g], T. Mersmann [a], M. Mielke [a], S. Mikirtychiants [b], H. Ohm [c], M. Papenbrock [a], M.N. Platonova [e], D. Prasuhn [c], V. Serdyuk [c], H. Ströher [c], A. Täschner [a], Yu. Valdau [c,b], C. Wilkin [h]

[a] Institut für Kernphysik, Westfälische Wilhelms-Universität Münster, Wilhelm-Klemm-Str. 9, 48149 Münster, Germany
[b] High Energy Physics Department, St. Petersburg Nuclear Physics Institute, RU-188350 Gatchina, Russia
[c] Institut für Kernphysik, Forschungszentrum Jülich, D-52425 Jülich, Germany
[d] Laboratory of Nuclear Problems, JINR, RU-141980 Dubna, Russia
[e] Skobeltsyn Institute of Nuclear Physics, Lomonosov Moscow State University, Leninskie Gory 1/2, 119991 Moscow, Russia
[f] H. Niewodniczanski Institute of Nuclear Physics PAN, PL-31342 Cracow, Poland
[g] High Energy Physics Institute, Tbilisi State University, GE-0186 Tbilisi, Georgia
[h] Physics and Astronomy Department, UCL, Gower Street, London WC1E 6BT, United Kingdom

ARTICLE INFO

Article history:
Received 1 June 2018
Received in revised form 12 July 2018
Accepted 24 July 2018
Available online 6 August 2018
Editor: V. Metag

Keywords:
Deuteron–proton elastic scattering
Glauber model

ABSTRACT

New precise unpolarised differential cross sections of deuteron–proton elastic scattering have been measured at 16 different deuteron beam momenta between $p_d = 3120.17$ MeV/c and $p_d = 3204.16$ MeV/c at the COoler SYnchrotron COSY of the Forschungszentrum Jülich. The data, which were taken using the magnetic spectrometer ANKE, cover the equivalent range in proton kinetic energies from $T_p = 882.2$ MeV to $T_p = 918.3$ MeV. The experimental results are analysed theoretically using the Glauber diffraction model with accurate nucleon–nucleon input. The theoretical cross section at $T_p = 900$ MeV agrees very well with the experimental one at low momentum transfers t. There are, however, significant deviations for $|t| > 0.2$ (GeV/c)^2 that must be investigated further.

1. Introduction

Deuteron–proton scattering is extensively used in the study of, e.g., meson production mechanisms in few-nucleon systems at intermediate energies. For such experiments dp elastic scattering is well suited for normalisation purposes, due to its high cross section over a large momentum transfer range (cf. Fig. 1). Previous work on meson production, e.g., Refs. [1–3], used the existing database [4–8] for data normalisation, assuming that for low momentum transfers, i.e., $|t| < 0.4$ (GeV/c)^2, the differential cross section as a function of t is independent of the beam momentum in the measured proton kinetic energy range between $T_p = 641$ MeV and $T_p = 1000$ MeV. This assumption was justified empirically by the fact that the available data do not show significant discrepancies in the slope of the differential cross sections. However analysis of individual experiments carried out by the same group at different energies (e.g., [7] at 793, 890, and 991 MeV and [8] at 641 and 793 MeV) shows only a slight energy dependence of the cross section at low momentum transfers, but which becomes more prominent as the momentum transfer grows.

Within the Glauber [9] or extended multiple scattering schemes (see, e.g., [10,11] and references therein) it is quite easy to understand the weak energy dependence of $d\sigma/dt$. The dominant term at small $|t|$ depends primarily on the pp and np total cross sections, which are almost constant between 800 and 1000 MeV [12]. In addition, most of the dependence on $|t|$ arises from the deuteron size, i.e., the deuteron wave function. There are less important effects coming, for example, from the energy dependence of the NN slope parameters, the relative real parts, and the spin-

* Corresponding author.
E-mail address: c.fritzsch@uni-muenster.de (C. Fritzsch).

https://doi.org/10.1016/j.physletb.2018.07.045

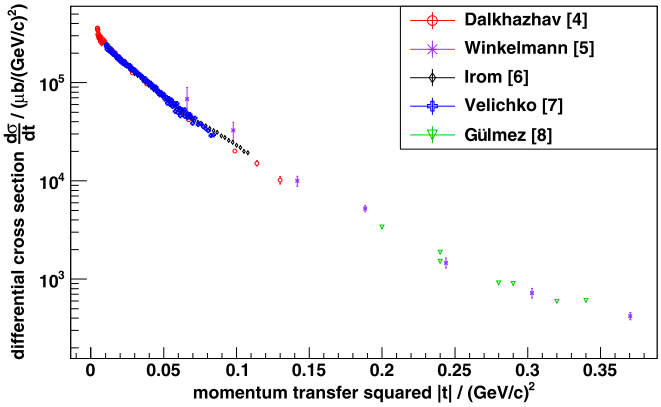

Fig. 1. Unpolarised differential cross sections of dp elastic scattering plotted as a function of the magnitude of the momentum transfer squared $|t|$ for different data sets [4–8].

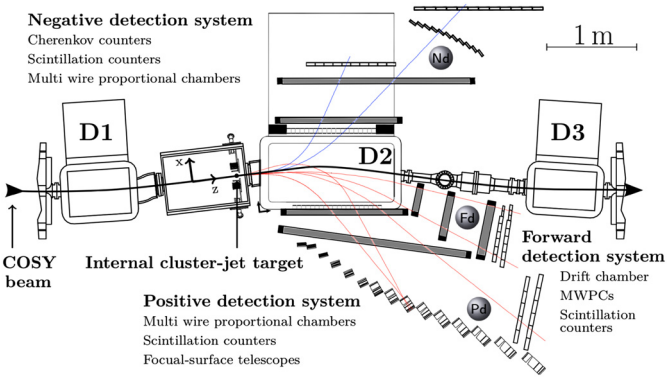

Fig. 2. Schematic view of the ANKE magnetic spectrometer. It mainly consists of three dipole magnets, an internal hydrogen cluster jet-target and three detection systems (Pd-, Nd- and Fd-system). The red lines represent possible tracks of positively charged particles and the blue lines of negatively charged particles. (For interpretation of the colours in the figure(s), the reader is referred to the web version of this article.)

dependent terms. If we neglect such effects, the limited energy dependence of the NN input is the primary physics reason for the weak energy dependence shown in Fig. 1. The same arguments apply for the pd total cross section [12], which is almost constant in our energy regime.

In contrast to the database at small momentum transfers $|t| < 0.1$ (GeV/c)^2, that at larger $|t|$ is much poorer. To be able to give a definitive answer as to what extent the differential cross section can be assumed to be energy-independent, one needs very precise measurements and also reliable theoretical predictions over a range of energies. High-precision data from the ANKE spectrometer, using a deuteron beam and a hydrogen target, allow further study of the behaviour of the unpolarised differential cross sections. This enlarges the database in the momentum transfer range $0.08 < |t| < 0.26$ (GeV/c)^2 at deuteron momenta that correspond to proton energies between $T_p = 882.2$ MeV and $T_p = 918.3$ MeV. This is, of course, a smaller range of energies than those shown in Fig. 1.

On the theoretical side, pd elastic scattering in the GeV energy region has usually been analysed in terms of the Glauber diffraction model (or its various extensions), which is a high-energy and low-momentum-transfer approximation to the exact multiple-scattering series for the hadron-nucleus scattering amplitude. The original Glauber model [9], where spin degrees of freedom were neglected (or included only partially), has been refined [10,11] by taking fully into account the spin structure of colliding particles, i.e., the spin-dependent NN amplitudes and the D-wave component of the deuteron wave function, and also the double-charge-exchange process $p + d \to n + (pp) \to p + d$. In addition, while the majority of previous calculations made within the Glauber model employed simple parameterisations for the forward NN amplitudes, the refined model [10,11] suggests using accurate NN amplitudes, based on modern NN partial-wave analysis (PWA). By using the NN PWA of the George Washington University SAID group (SAID) [13], the model has been shown to describe small-angle pd differential cross sections and also the more sensitive polarisation observables very well in the energy range $T_p = 200$–1000 MeV [10]. The refined Glauber model therefore seems ideally suited for the description of the experimental data presented here. On the other hand, the new high-precision data can provide a precise test for applicability of the Glauber model.

The SAID group has recently published an updated NN PWA solution [14], which incorporates the new COSY-ANKE data on the near-forward cross section [15] and analysing power A_y [16] in pp elastic scattering, as well as the recent COSY-WASA A_y data in np elastic scattering [17]. We can therefore re-examine the predictions of the refined Glauber model obtained with the use of the previous PWA solution of 2007 [13]. By performing calculations at various incident energies from 800 to 1000 MeV, we can also test the widely-used assumption of energy independence of the pd elastic differential cross section at low momentum transfers.

Table 1
Beam momenta p_d for each supercycle and flattop in MeV/c.

	FT1	FT2	FT3	FT4	FT5	FT6	FT7
SC1	3120.17	3146.41	3148.45	3152.45	3158.71	3168.05	3177.51
SC2	3120.17	3147.35	3150.42	3154.49	3162.78	3172.15	3184.87
SC3				3157.48	3160.62		3204.16

2. Experimental setup

The data were taken with the magnetic spectrometer ANKE [18] (cf. Fig. 2 for a schematic representation of the layout), which is part of an internal fixed-target experimental setup located at the COoler SYnchrotron (COSY) of the Forschungszentrum Jülich. One of the main components of ANKE is the magnetic system, with its three dipole magnets D1–D3. The accelerated beam of unpolarized deuterons is deflected by the first dipole magnet D1 (cf. Fig. 2) into the target chamber, where the beam interacts with the internal hydrogen cluster-jet target [19].

The second dipole magnet D2 separates the ejectiles by their charge and momentum into three different detection systems. The deuterons associated with dp elastic scattering are deflected by D2 into the Forward (Fd) detector, which was the only element used in this experiment. The Fd was designed and installed near the beam pipe to detect high-momentum particles. Beam particles not interacting with the internal target are deflected by the dipole magnets D2 and D3 back onto the nominal ring orbit. A special feature of this magnetic spectrometer is the moveable D2 magnet, which can be shifted perpendicular to the beam line. It is thus possible to optimise the geometrical acceptance of the detection system for the particular reaction that one would like to investigate. The deuteron beam momentum range from 3120.17 MeV/c to 3204.16 MeV/c was divided into 16 different fixed beam momenta (cf. Table 1, originally for the determination of the η meson mass [20]) using the supercycle mode of COSY. In each supercycle it is possible to alternate between up to seven different beam settings, each with a cycle length of 206 s. The beam momentum spread $\Delta p_\mathrm{d}/p_\mathrm{d} < 6 \times 10^{-5}$ was determined using the spin-depolarisation technique [21].

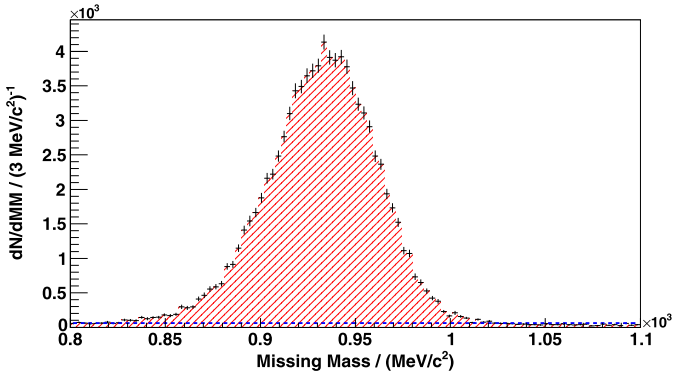

Fig. 3. Missing-mass spectrum of the $dp \to dX$ reaction at $p_d = 3120.17$ MeV/c for $0.08 < |t| < 0.09$ (GeV/c)^2. The blue dashed line represents a constant background fit to the spectrum, excluding the $\pm 3\sigma$ region around the peak.

3. Event selection and analysis

As described above, deuterons originating from dp elastic scattering are deflected by D2 into the Forward detection system, which consists of one multiwire drift chamber and two multiwire proportional chambers for track reconstruction. In addition, two scintillator hodoscopes, comprised of eight vertically aligned scintillator strips for the first and nine for the second hodoscope, are used for particle identification on the basis of the energy-loss information and time-of-flight measurements. During the data taking a specific hardware trigger was included, which required two coincident scintillator signals, one in each of the two Fd hodoscopes. Due to the cross section for dp elastic scattering being very large, this hardware trigger is equipped with a pre-scaling factor of 1024 to reduce the dead time of the data acquisition system. On account of the small momentum transfer to the target proton, the forward-going deuterons, whose tracks are reconstructed in the Forward detector, have momenta close to that of the beam. Since only deuterons from elastic scattering have such high momenta, the reaction can be identified with no physical background from meson production. Particles with a reconstructed momentum p below about $p/p_d \approx 0.913$ are discarded to obtain a better signal-to-noise ratio. In order to avoid uncertainties caused by small inhomogeneities of the magnetic field at the edges of the D2 magnet, an additional cut in the y hit position (with y being the axis perpendicular to the COSY plane) of the first multi-wire proportional chamber is required. Events with $|y_{\mathrm{hit}}| > 105$ mm are discarded. For dp elastic scattering the geometrical acceptance of the ANKE magnetic spectrometer is limited to $0.06 < |t| < 0.31$ (GeV/c)^2. However, to avoid systematic edge effects, only events in the region $0.08 < |t| < 0.26$ (GeV/c)^2 were analysed, with a bin width of $\Delta t = 0.01$ (GeV/c)^2. The missing-mass analysis of Fig. 3 shows a prominent signal at the proton mass sitting on top of a very small and seemingly constant background.

A Gaussian fit to the peak was used to define its position and width and the region outside the $\pm 3\sigma$ region was used to fit a constant background. After subtracting this, the missing-mass spectra were summed to obtain the number of dp elastic scattering events for each of the 18 momentum transfer bins at all 16 different beam momenta. The detector acceptance, which drops from 15% to 7% with increasing momentum transfer, was determined from Monte Carlo simulations. These simulations have to fulfil the same software cut criteria as the data, so that the acceptance-corrected count yield can be determined for each beam momentum setting. The resulting differential cross sections are presented in Sec. 5.

4. Theoretical calculation

The theoretical calculation of the pd elastic scattering cross section was performed at four incident proton energies $T_p = 800$, 900, 950 and 1000 MeV within the refined Glauber model [10,11]. The differential cross section is related to the amplitude M as

$$\mathrm{d}\sigma/\mathrm{d}t = \tfrac{1}{6}\mathrm{Sp}\left(MM^{+}\right). \tag{1}$$

The pd amplitude M in the Glauber approach contains terms corresponding to single and double scattering of the projectile with the nucleons in the deuteron. These terms are expressed through the on-shell NN amplitudes (pp amplitude M_p and pn amplitude M_n) and the deuteron wave function Ψ_d:

$$M(\mathbf{q}) = M^{(s)}(\mathbf{q}) + M^{(d)}(\mathbf{q}), \tag{2}$$

$$M^{(s)}(\mathbf{q}) = \int \mathrm{d}^3 r\, e^{i\mathbf{q}\mathbf{r}/2}\Psi_d(\mathbf{r})\left[M_n(\mathbf{q}) + M_p(\mathbf{q})\right]\Psi_d(\mathbf{r}), \tag{3}$$

$$M^{(d)}(\mathbf{q}) = \frac{i}{4\pi^{3/2}}\int \mathrm{d}^2 q' \int \mathrm{d}^3 r\, e^{i\mathbf{q}'\mathbf{r}}\Psi_d(\mathbf{r}) \times \tag{4}$$

$$\left[M_n(\mathbf{q_2})M_p(\mathbf{q_1}) + M_p(\mathbf{q_2})M_n(\mathbf{q_1}) - M_c(\mathbf{q_2})M_c(\mathbf{q_1})\right]\Psi_d(\mathbf{r}),$$

where $\mathbf{q}$ is the overall 3-momentum transfer (so that $t = -q^2$ in the centre-of-mass system), while $\mathbf{q_1} = \mathbf{q}/2 - \mathbf{q}'$ and $\mathbf{q_2} = \mathbf{q}/2 + \mathbf{q}'$ are the momenta transferred in collisions with individual target nucleons, and $M_c(\mathbf{q}) = M_n(\mathbf{q}) - M_p(\mathbf{q})$ is the amplitude of the charge-exchange process $pn \to np$.

When spin dependence is taken into account, the NN amplitudes M_n, M_p and the deuteron wave function Ψ_d are non-commuting operators in the three-nucleon spin space. They can be written in terms of independent elements that are invariant under spatial rotations and space and time reflections, and the coefficients of the expansions are the NN invariant amplitudes (five for both pp and pn scattering) and the S- and D-wave components of the deuteron wave function. The pd amplitude M is also expanded into 12 independent terms. After undertaking some spin algebra and integrating over the spatial coordinate, all the pd invariant amplitudes can be explicitly related to the NN invariant amplitudes and the various components of the deuteron form factor $S(\mathbf{q}) = \int \mathrm{d}^3 r\, e^{i\mathbf{q}\mathbf{r}}|\Psi_d(\mathbf{r})|^2$. The detailed derivation and the final formulae of the refined Glauber model can be found in Refs. [10, 11].

The NN invariant amplitudes at low momentum transfers are readily evaluated from the centre-of-mass helicity amplitudes, which can be constructed from empirical NN phase shifts. For the present calculation, we used the phase shifts of the latest PWA solution of the SAID group [14]. There are, in fact, two PWA solutions published in Ref. [14], viz. the unweighted fit SM16 and the weighted fit WF16. Unlike their earlier solution SP07 [13], both new SAID solutions incorporate the recent high-precision COSY-ANKE data [15,16] on the near-forward differential cross section ($1.0 \le T_p \le 2.8$ GeV) and analysing power A_y ($0.8 \le T_p \le 2.4$ GeV) in pp elastic scattering and the COSY-WASA data [17] on A_y in np scattering at $T_n = 1.135$ GeV. By construction, the WF16 solution describes better the new COSY-ANKE results since the weights of these data are here enhanced.

The NN partial-wave amplitudes obtained in the SM16, WF16 and SP07 solutions begin to deviate significantly from each other only for $T_p > 1$ GeV. We examined both new PWA solutions at $T_p = 900$ MeV and found the pd differential cross section with WF16 input to be lower than that produced by SM16 by between 1% and 3% for $0.08 < |t| < 0.26$ (GeV/c)^2. This small difference is some measure of the uncertainties arising from the input on-shell NN amplitudes. For three other energies ($T_p = 800$, 950,

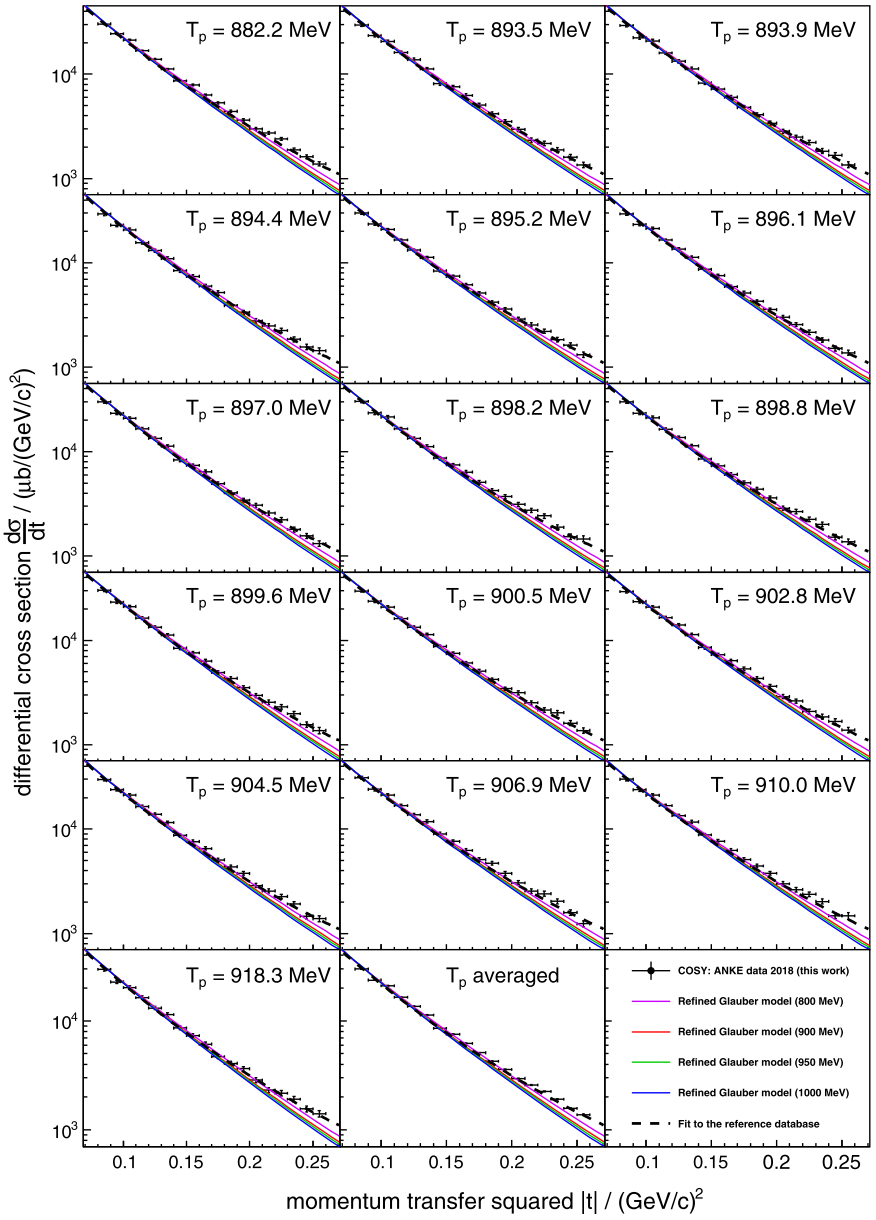

Fig. 4. Differential cross sections for deuteron–proton elastic scattering for deuteron laboratory momenta between 3120.17 and 3204.16 MeV/c. These are labelled in terms of the proton kinetic energy for a deuteron target ($882.2 \leq T_p \leq 918.3$ MeV). Also shown is the average over the 16 available measurements. The purple ($T_p = 800$ MeV), red ($T_p = 900$ MeV), green ($T_p = 950$ MeV), and blue ($T_p = 1000$ MeV) lines represent the refined Glauber model calculations (with the use of the SAID NN PWA, solution WF16 [14]) and the dashed black line the fit to the dp-elastic database from [4–8].

and 1000 MeV) we employed the WF16 NN PWA solution and at $T_p = 1000$ MeV we also compared the results with those obtained with the SP07 input used in earlier works [10,11]. The changes ranged from 1% to 8% in the momentum transfer interval $0.08 < |t| < 0.26$ (GeV/c)^2.

Due to the rapid fall-off of the NN amplitudes with momentum transfer, the pd predictions in the Glauber model are sensitive mainly to the long-range behaviour of the deuteron wave function. We used that derived from the CD-Bonn NN-potential [22]. Choosing a different (but realistic) wave function would change the resulting pd predictions by not more than a few percent [11].

The dependence of the NN helicity amplitudes on the momentum transfer q, as well as that of the deuteron S- and D-wave functions on the inter-nucleon distance r, were conveniently parameterised in terms of five-Gaussians, which allows us to perform all the calculations fully analytically [10,11]. The fitted NN amplitudes coincide with the SAID input at momentum transfers $q < 0.7$ GeV/c and the deuteron wave functions at distances $r < 20$ fm.

5. Results

The normalisation of the data presented here is obtained using the fit

$$\mathrm{d}\sigma/\mathrm{d}t = \exp(a + b|t| + c|t|^2)\ \mu\mathrm{b}/(\mathrm{GeV}/c)^2 \qquad (5)$$

in the momentum transfer range $0.05 < |t| < 0.4$ (GeV/c)^2 to the combined database from Refs. [4–8]. This yields the parameters $a = 12.45$, $b = -27.24$ (GeV/c)$^{-2}$ and $c = 26.31$ (GeV/c)$^{-4}$. To normalise the acceptance-corrected counts at each beam momentum, both the fit to the reference database, as well as the numbers of counts, are integrated over the momentum transfer range

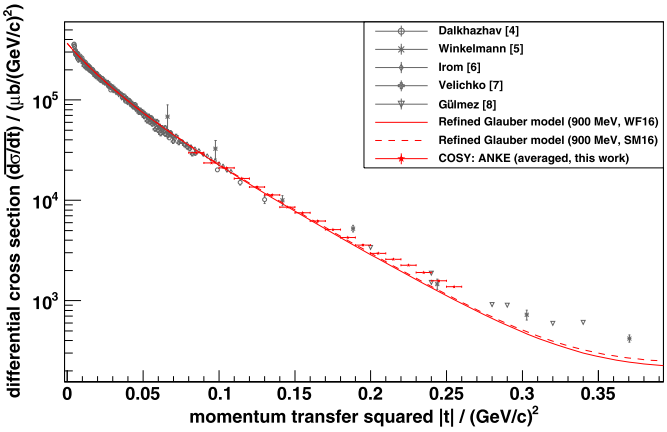

Fig. 5. Differential cross sections $\overline{d\sigma/dt}$ averaged over the available 16 energies between 882.2 MeV $\leq T_p \leq$ 918.3 MeV compared with the existing database [4–8] and the predictions of the refined Glauber model at $T_p = 900$ MeV obtained using the SAID *NN* PWA solutions WF16 and SM16 [14].

Table 2
Differential cross section $\overline{d\sigma/dt}$ and statistical uncertainty of *dp* elastic scattering averaged over all 16 different beam momenta.

$\|t\|$ (GeV/c)^2	$\overline{d\sigma/dt}$ μb/(GeV/c)^2	$\Delta\overline{d\sigma/dt}_{stat}$ μb/(GeV/c)^2
0.085	29898	193
0.095	23624	155
0.105	21014	140
0.115	16448	112
0.125	13562	95
0.135	11295	82
0.145	8546	65
0.155	7534	59
0.165	6212	51
0.175	5098	45
0.185	4264	39
0.195	3575	35
0.205	2963	31
0.215	2573	29
0.225	2249	26
0.235	1909	24
0.245	1575	21
0.255	1379	20

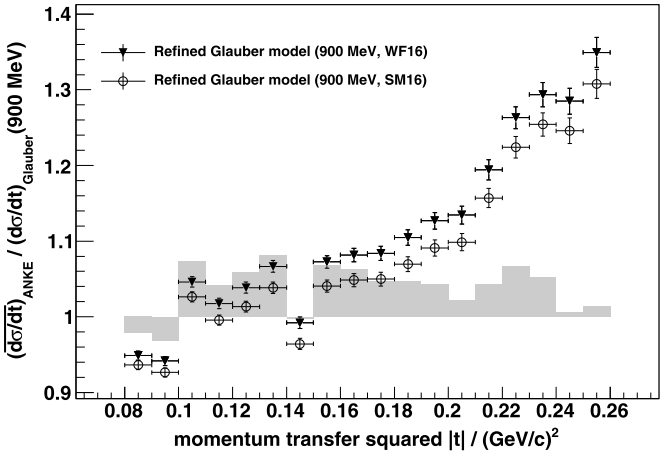

Fig. 6. Ratio of our measured differential cross sections $\overline{d\sigma/dt}$ averaged over the available 16 energies to the predictions of the refined Glauber model at $T_p =$ 900 MeV obtained using the SAID *NN* PWA solutions WF16 and SM16 [14]. The grey bars represent the ratio of the averaged differential cross sections to the fit to the reference database.

$0.08 < |t| < 0.09$ (GeV/c)^2. Assuming $d\sigma/dt$ is independent of the beam momentum, the ratio between the two integrals defines the scaling factor for each beam momentum that takes into account, e.g., different integrated luminosities. The differential cross sections thus determined in this way are shown in Fig. 4 for all 16 beam momenta. The plots of differential cross sections at the different beam momenta show that their t-dependence is independent of beam momentum over the available momentum range. As a consequence, it is possible to evaluate the differential cross section for each of the 18 momentum transfer bins averaged over the 16 energies (cf. Fig. 4, Fig. 5, and Table 2). The systematic uncertainties caused by, e.g., the uncertainty in the angle calibration in the D2 magnet are negligible compared to the statistical uncertainties that are presented in Table 2. From the comparison of the results with the theoretical calculation at $T_p = 900$ MeV (see Figs. 4 and 5), it is seen that the refined Glauber model describes our data very well at low momentum transfers $0.08 < |t| < 0.2$ (GeV/c)^2. It is also evident from Fig. 5 that the refined Glauber model calculation agrees similarly with the existing database for $|t| < 0.1$ (GeV/c)^2. Fig. 6 shows the ratio of the averaged cross section determined in the present experiment to that calculated within the refined Glauber model. The scatter of this ratio around unity for $0.08 < |t| < 0.18$ (GeV/c)^2 is consistent with the scatter of experimental data around the smooth curve fitting the reference database (see Fig. 6).

At the higher momentum transfers, the theoretical curve begins to deviate from experiment and this may be due to a failure of the small-momentum-transfer approximations (account of only single and double scattering, neglect of recoil, etc.) involved in the Glauber theory. On the other hand, it was found in Ref. [10] that at the lower energies of $T_p = 250$ and 440 MeV the refined Glauber model calculations agree with the data on *pd* elastic differential cross section out to at least $|t| = 0.3$ (GeV/c)^2, i.e., in the same region where exact three-body Faddeev equations describe the data. However, the Glauber model is a high-energy approximation to the exact theory and its accuracy should get better at higher collision energy. The deviations noted here for $|t| > 0.2$ (GeV/c)^2 might arise from dynamical mechanisms that are not taken into account in either the approximate (Glauber-like) or the exact (Faddeev-type) approach. For example, there could be contributions from a three-nucleon ($3N$) force whose importance rises with collision energy and momentum transfer. One conventional $3N$-force, induced by two-pion exchange with an intermediate $\Delta(1232)$-isobar excitation, is known to contribute to *pd* large-angle scattering at intermediate energies (see, e.g., [23]). However, one might also consider three-body forces caused by the meson exchange between

the proton and the six-quark core of the deuteron (the deuteron dibaryon) [24]. Indeed, at larger momentum transfers, the incident proton probes shorter NN distances in the deuteron, so that, the proton scattering off the deuteron as a whole could occur with increasing probability. The preliminary results of taking the one-meson-exchange between the incident proton and deuteron dibaryon into account in pd elastic scattering have shown this $3N$-force contribution to increase slightly the pd differential cross section already at moderate momentum transfers [25]. This interesting question clearly requires further investigation.

The calculations at different proton energies from 800 to 1000 MeV show a gradual energy dependence of the pd differential cross section (see Fig. 4). The theoretical curves at four energies intersect at around $|t| = 0.08$ (GeV/c)^2 before beginning to diverge from each other. The difference between the calculated cross sections at $T_p = 800$ and 1000 MeV reaches 13% at $|t| = 0.2$ (GeV/c)^2. Hence, in the energy range covered by the present experiment, i.e., from 882.2 to 918.3 MeV, the maximum difference in the pd differential cross section is only 2–3% at the highest available momentum transfers. This small deviation lies within the uncertainty related to the input NN amplitudes and thus can be neglected. The new data are completely consistent with the assumption that the energy dependence is negligible over the range $882.2 < T_p < 918.3$ MeV. On the other hand, some of the older data obtained over a wider energy range (e.g., [7] at 793, 890, and 991 MeV and [8] at 641 and 793 MeV) show a weak energy dependence of the cross section which, at least qualitatively, agrees with our theoretical predictions.

The energy dependence found in the Glauber model calculations comes from a similar energy behaviour of the NN differential cross sections obtained in the SAID PWA, which describes properly the NN elastic database. The increasing slope of the curve implies that in our energy region the interaction radius in pd (as well as NN) elastic scattering effectively increases with energy. As a result, the forward diffraction peak becomes higher and narrower. This means that the pd elastic cross section integrated over $0 < |t| < 0.2$ (GeV/c)^2 increases slightly with energy in our model calculations (by approximately 4% from 800 to 1000 MeV), though the part taken from $|t| = 0.08$ (GeV/c)^2 (the lower limit of the present experiment) decreases a little. Hence, whereas the pd elastic cross section as a function of the momentum transfer squared is usually assumed to be constant in the energy and momentum-transfer range considered, the present model calculations reveal a slight energy dependence of the magnitude and slope of the pd elastic cross section. This result has already been taken into account for normalisation of the recent COSY-WASA experimental data on the η-meson production in pd collisions [26].

6. Summary

Due to its small number of active particles, deuteron–proton scattering at intermediate energies is well suited for the study of various non-standard mechanisms of hadron interaction, such as the production of nucleon isobars, dibaryon resonances, etc. However, even for dp elastic scattering, the experimental database is scarce at momentum transfers $|t| > 0.1$ (GeV/c)^2. In this work, new precise measurements of the differential cross sections for dp elastic scattering at 16 equivalent proton energies between $T_p = 882.2$ MeV and $T_p = 918.3$ MeV in the range $0.08 < |t| < 0.26$ (GeV/c)^2 have been presented. Since the shapes of the differential cross sections were found to be independent of beam momentum, it was possible to determine precise average values over the whole momentum transfer range.

The experimental data at low momentum transfers are well described by the refined Glauber approach at an average energy $T_p = 900$ MeV. These calculations take full account of spin degrees of freedom and use accurate input NN amplitudes based on the most recent partial-wave analysis of the SAID group [14]. However, as is seen very evidently from Fig. 5, there are clear deviations between the data and the theoretical predictions for $|t| > 0.2$ (GeV/c)^2. Such deviations, which are likely to be due to failure of the small-momentum-transfer approximations involved in the Glauber model, must be investigated further since they might also reflect the missing contributions of some dynamical mechanisms such as $3N$ forces.

The calculations at different energies, i.e., $T_p = 800$, 900, 950, and 1000 MeV, reveal a slight energy dependence (increasing slope) in the pd elastic cross section as a function of the momentum transfer squared $|t|$. The predicted energy dependence arises mainly from the similar energy behaviour of the input NN elastic cross sections. For pd scattering, it may be trusted only in the small momentum transfer region $|t| < 0.2$ (GeV/c)^2 where the refined Glauber model describes the data. This behaviour has to be taken into account when using pd elastic scattering in the normalisation of other experimental data. However, the energy dependence found in this region is very weak. In fact, there are clear physical reasons mentioned in the Introduction for the relative stability of the pd elastic cross section at low momentum transfers in our energy regime. Thus, the slight change of the slope predicted by the Glauber model would be hardly visible over the whole energy range from 641 to 1000 MeV covered by the existing database [4–8]. This is even more true for the 36 MeV energy range studied here. However, some energy dependence which coincides qualitatively with our predictions might be identified in some of the older experiments [7,8] and it would be highly desirable to perform very precise measurements of the pd differential cross section as a function of t in a wider energy range than that covered by the present experiment.

In addition to the unpolarised differential cross sections, it would be interesting to study the momentum transfer and energy behaviour of polarisation observables (analysing powers, etc.), which can readily be calculated within the refined Glauber model at the same energies $T_p = 800$–1000 MeV. The theoretical predictions for such observables will be presented in a forthcoming paper.

Acknowledgements

We are grateful to other members of the ANKE collaboration and the COSY crew for their work and the good experimental conditions during the beam time. This work has been supported by the JCHP FFE No. 41808260, by the DFG through the Research Training Group GRK2149, and by the Russian Foundation for Basic Research, grant No. 16-02-00265.

References

[1] T. Mersmann, et al., Phys. Rev. Lett. 98 (2007) 242301, https://doi.org/10.1103/PhysRevLett.98.242301, arXiv:nucl-ex/0701072.
[2] T. Rausmann, et al., Phys. Rev. C 80 (2009) 017001, https://doi.org/10.1103/PhysRevC.80.017001, arXiv:0905.4595.
[3] M. Mielke, et al., Eur. Phys. J. A 50 (2014) 102, https://doi.org/10.1140/epja/i2014-14102-2, arXiv:1404.2066.
[4] N. Dalkhazhav, et al., Sov. J. Nucl. Phys. 8 (1969) 196–202, Yad. Fiz. 8 (1968) 342.
[5] E. Winkelmann, et al., Phys. Rev. C 21 (1980) 2535–2541, https://doi.org/10.1103/PhysRevC.21.2535.
[6] F. Irom, et al., Phys. Rev. C 28 (1983) 2380–2385, https://doi.org/10.1103/PhysRevC.28.2380.
[7] G.N. Velichko, et al., Sov. J. Nucl. Phys. 47 (1988) 755–759, Yad. Fiz. 47 (1988) 1185.
[8] E. Guelmez, et al., Phys. Rev. C 43 (1991) 2067–2076, https://doi.org/10.1103/PhysRevC.43.2067.

[9] V. Franco, R.J. Glauber, Phys. Rev. 142 (1966) 1195–1214, https://doi.org/10.1103/PhysRev.142.1195.
[10] M.N. Platonova, V.I. Kukulin, Phys. Rev. C 81 (2010) 014004, https://doi.org/10.1103/PhysRevC.81.014004, arXiv:1612.08694; Erratum: Phys. Rev. C 94 (6) (2016) 069902, https://doi.org/10.1103/PhysRevC.94.069902.
[11] M.N. Platonova, V.I. Kukulin, Phys. At. Nucl. 73 (2010) 86–106, https://doi.org/10.1134/S1063778810010114, Yad. Fiz. 73 (2010) 90.
[12] D.V. Bugg, D.C. Salter, G.H. Stafford, R.F. George, K.F. Riley, R.J. Tapper, Phys. Rev. 146 (1966) 980–992, https://doi.org/10.1103/PhysRev.146.980.
[13] R.A. Arndt, W.J. Briscoe, I.I. Strakovsky, R.L. Workman, Phys. Rev. C 76 (2007) 025209, https://doi.org/10.1103/PhysRevC.76.025209, arXiv:0706.2195.
[14] R.L. Workman, W.J. Briscoe, I.I. Strakovsky, Phys. Rev. C 94 (2016) 065203, https://doi.org/10.1103/PhysRevC.94.065203, arXiv:1609.01741.
[15] D. Mchedlishvili, et al., Phys. Lett. B 755 (2016) 92–96, https://doi.org/10.1016/j.physletb.2016.01.066, arXiv:1510.06162.
[16] Z. Bagdasarian, et al., Phys. Lett. B 739 (2014) 152–156, https://doi.org/10.1016/j.physletb.2014.10.054, arXiv:1409.8445.
[17] P. Adlarson, et al., WASA-at-COSY, Phys. Rev. Lett. 112 (2014) 202301, https://doi.org/10.1103/PhysRevLett.112.202301, arXiv:1402.6844.
[18] S. Barsov, et al., ANKE, Nucl. Instrum. Methods A 462 (2001) 364–381, https://doi.org/10.1016/S0168-9002(00)01147-5.
[19] A. Khoukaz, et al., Eur. Phys. J. D 5 (1999) 275.
[20] P. Goslawski, et al., Phys. Rev. D 85 (2012) 112011, https://doi.org/10.1103/PhysRevD.85.112011, arXiv:1204.3520.
[21] P. Goslawski, et al., Phys. Rev. Spec. Top., Accel. Beams 13 (2010) 022803, https://doi.org/10.1103/PhysRevSTAB.13.022803, arXiv:0908.3103.
[22] R. Machleidt, Phys. Rev. C 63 (2001) 024001, https://doi.org/10.1103/PhysRevC.63.024001, arXiv:nucl-th/0006014.
[23] K. Sekiguchi, et al., Phys. Rev. C 89 (2014) 064007, https://doi.org/10.1103/PhysRevC.89.064007.
[24] V.I. Kukulin, V.N. Pomerantsev, M. Kaskulov, A. Faessler, J. Phys. G 30 (2004) 287–308, https://doi.org/10.1088/0954-3899/30/3/005, arXiv:nucl-th/0308059.
[25] M.N. Platonova, V.I. Kukulin, J. Phys. Conf. Ser. 381 (2012) 012110, https://doi.org/10.1088/1742-6596/381/1/012110.
[26] P. Adlarson, et al., WASA-at-COSY, Phys. Lett. B 782 (2018) 297–304, https://doi.org/10.1016/j.physletb.2018.05.036, arXiv:1801.06671.